

## Humanized Anti-CD26 Monoclonal Antibody as a Treatment for Malignant Mesothelioma Tumors

Teruo Inamoto,<sup>1,3</sup> Taketo Yamada,<sup>2</sup> Kei Ohnuma,<sup>1</sup> Shinichiro Kina,<sup>1</sup> Nozomu Takahashi,<sup>1</sup> Tadanori Yamochi,<sup>1</sup> Sakiko Inamoto,<sup>1,3</sup> Yoji Katsuoka,<sup>3</sup> Osamu Hosono,<sup>1</sup> Hirotohi Tanaka,<sup>1</sup> Nam H. Dang,<sup>4</sup> and Chikao Morimoto<sup>1,4</sup>

**Abstract Purpose:** CD26 is a 110-kDa cell surface antigen with a role in tumor development. In this report, we show that CD26 is highly expressed on the cell surface of malignant mesothelioma and that a newly developed humanized anti-CD26 monoclonal antibody (mAb) has an inhibitory effect on malignant mesothelioma cells in both *in vitro* and *in vivo* experiments.

**Experimental Design:** Using immunohistochemistry, 12 patients' surgical specimens consisting of seven malignant mesothelioma, three reactive mesothelial cells, and two adenomatoid tumors were evaluated for expression of CD26. The effects of CD26 on malignant mesothelioma cells were assessed in the presence of transfection of CD26-expressing plasmid, humanized anti-CD26 mAb, or small interfering RNA against CD26. The *in vivo* growth inhibitory effect of humanized anti-CD26 mAb was assessed in human malignant mesothelioma cell mouse xenograft models.

**Results:** In surgical specimens, CD26 is highly expressed in malignant mesothelioma but not in benign mesothelial tissues. Depletion of CD26 by small interfering RNA results in the loss of adhesive property, suggesting that CD26 is a binding protein to the extracellular matrix. Moreover, our *in vitro* data indicate that humanized anti-CD26 mAb induces cell lysis of malignant mesothelioma cells via antibody-dependent cell-mediated cytotoxicity in addition to its direct anti-tumor effect via p27<sup>kip1</sup> accumulation. *In vivo* experiments with mouse xenograft models involving human malignant mesothelioma cells show that humanized anti-CD26 mAb treatment drastically inhibits tumor growth in tumor-bearing mice, resulting in enhanced survival.

**Conclusions:** Our data strongly suggest that humanized anti-CD26 mAb treatment may have potential clinical use as a novel cancer therapeutic agent in CD26-positive malignant mesothelioma.

Malignant mesothelioma is an aggressive cancer arising from the mesothelial cells lining the pleura. It is usually associated with the history of chronic asbestos exposure (1). Because of the long latency period between asbestos exposure and tumor development, the annual incidence of 2,500 new cases in the

United States is expected to increase by >50% in the coming decade (2). Moreover, incidence world wide is projected to increase substantially in the next decades (3). The prognosis is very poor with a median survival of 4 to 12 months despite the therapies currently used, including surgery, radiotherapy, and chemotherapy (4). Because of the inefficacy of the conventional treatments, novel therapeutic strategies are urgently needed to be developed.

CD26 is a 110-kDa surface glycoprotein with dipeptidyl peptidase IV activity able to cleave selected biological factors to alter their functions (5). CD26/dipeptidyl peptidase IV is involved in T-lymphocyte costimulation and signal transduction processes (6, 7) and regulates topoisomerase II  $\alpha$  level in hematologic malignancies, affecting sensitivity to doxorubicin and etoposide (8). Expressed on various tissues (4, 9), CD26 is involved in the development of certain human cancers (9–12). CD26 is also known to serve as a binding motif for extracellular matrix (ECM) in human and rodents (13, 14). Previously, we reported that CD26 was collagen-binding protein using a CD26 positive JMN cell line, which is derived from malignant mesothelioma (15). Moreover, our previous works have shown that anti-CD26 monoclonal antibody (mAb) inhibits growth of CD26-positive T-cell malignancies (16, 17) and renal cell carcinoma (18).

**Authors' Affiliations:** <sup>1</sup>Division of Clinical Immunology, Advanced Clinical Research Center, Institute of Medical Science, University of Tokyo and <sup>2</sup>Department of Pathology, Keio University, Tokyo, Japan; <sup>3</sup>Department of Medicine, Osaka Medical College, Osaka, Japan; and <sup>4</sup>Department of Hematologic Malignancies, Nevada Cancer Institute, Las Vegas, Nevada  
Received 1/16/07; revised 3/14/07; accepted 3/22/07.

**Grant support:** Ministry of Education, Science, Sports, and Culture grant (K. Ohnuma and C. Morimoto), Ministry of Health, Labor, and Welfare, Japan (C. Morimoto), and Yasuda Medical Foundation (T. Inamoto).

The costs of publication of this article were defrayed in part by the payment of page charges. This article must therefore be hereby marked *advertisement* in accordance with 18 U.S.C. Section 1734 solely to indicate this fact.

**Conflict of interest:** Dr. Morimoto is a board member of Y's Therapeutics, and Dr. Dang is a scientific adviser in Y's Therapeutics. The other authors have no competing financial interests.

**Requests for reprints:** Chikao Morimoto, Division of Clinical Immunology, Advanced Clinical Research Center, Institute of Medical Science, University of Tokyo, 4-6-1, Shirokanedai, Minato-ku, Tokyo 108-8639, Japan. E-mail: morimoto@ims.u-tokyo.ac.jp.

© 2007 American Association for Cancer Research.  
doi:10.1158/1078-0432.CCR-07-0110

Our previous report shows that the murine anti-CD26 mAb 14D10, which recognizes the cell membrane-proximal glycosylated region starting with a 20-amino acid flexible stalk region of human CD26, has direct antitumor effect by inducing G<sub>1</sub>-S arrest while concomitantly blocking the adhesion of cancer cells to the ECM. However, another murine anti-CD26 mAb, termed 5F8, which detects the cysteine-rich domain of CD26, lacks this biological activity (18).

Because human malignant mesothelioma is a highly malignant tumor resistant to apparent conventional treatment, the detection of novel target and development of new treatment strategies in malignant mesothelioma are urgently needed (4, 19). In this report, we analyzed the expression of CD26 in the tissues of patients with malignant mesothelioma and validated the antitumor effect of a novel humanized anti-CD26 mAb which was constructed from high-affinity Fab clone to the 14D10 variable region by targeting malignant mesothelioma, hence concomitantly showing the functional role of CD26 in this neoplasm.

## Materials and Methods

**Reagents and antibodies.** Anti-CD26 mouse mAb (IgG1)14D10, 5F8, and anti-CD45RA mouse mAb (IgG1) 2H4 were developed in our laboratory as described previously (20, 21), with the last one being used as control. Normal human IgG1 (Sigma-Aldrich) was also used as a control. Humanized anti-CD26 mAb (IgG1 isotype) was constructed from 14D10 coding sequence (generously provided by Y's Therapeutics). Mouse mAb to PKB $\alpha$ /Akt, CDK2, CDK4, CDK6, cyclin E, and  $\beta$ -actin were from Cell Signaling Technology Inc., and mouse mAb to p27<sup>kip1</sup>, p21<sup>cip1/waf1</sup>, cyclin D1, and activated caspase-3 were from BD PharMingen. Antihuman IgG, Fc $\gamma$  fragment specific F(ab')<sub>2</sub> fragment of goat and anti-mouse IgG, Fc $\gamma$  fragment specific F(ab')<sub>2</sub> fragment of goat were from Jackson ImmunoResearch.

**Cell culture and transfection.** JMN cells were a kind gift from Dr. Brenda Gerwin (Laboratory of Human Carcinogenesis, NIH, Bethesda, MD). NCI-H2452 and 293T cells were obtained from the American Type Culture Collection. JMN and NCI-H2452 cell lines were derived from patients with malignant mesothelioma. All cells were grown in RPMI medium (Life Technologies Inc.) supplemented with 10% heat-inactivated fetal bovine serum, penicillin (100 units/mL), and streptomycin (100  $\mu$ g/mL; Life Technologies) or G418 (500  $\mu$ g/mL; Sigma-Aldrich). 293T cells were transfected with full-length CD26 subcloned into a pEB6 vector (22) using FuGENE6 reagent (Roche Diagnostics).

**2-(2-methoxy-4-nitrophenyl)-3-(4-nitrophenyl)-5-(2,4-disulfo-phenyl)-2H-tetrazolium assay.** Cells were subjected to incubation in 96-well plates in media alone or in the presence of humanized anti-CD26 mAb (0.1, 1.0, or 10  $\mu$ g/mL) or 2H4 (0.1, 1.0, or 10  $\mu$ g/mL) for a total volume of 100  $\mu$ L ( $5 \times 10^3$  cells per well). After 24 h of incubation at 37°C, 2-(2-methoxy-4-nitrophenyl)-3-(4-nitrophenyl)-5-(2,4-disulfo-phenyl)-2H-tetrazolium (Seikagaku) was added to each well. After another 2 h of incubation, water soluble formazan dye upon bioreduction in the presence of an electron carrier, 1-methoxy-5-methylphenazinium, was measured at 450 nm using a microplate reader (Bio-Rad). All samples were tested in triplicate. Values reported represent the means of triplicated wells, and SE was within 15.

**Immunohistochemistry.** For immunohistochemistry, 12 patients' surgical specimens consisting of seven malignant mesothelioma, three reactive mesothelial cells, and two adenomatoid tumors were evaluated. For each, 10% formalin-fixed, paraffin-embedded specimens, containing both the carcinoma and its adjacent nonneoplastic tissue, were prepared. Paraffin-embedded tissues were dewaxed and rehydrated

using xylene and ethanol, respectively. Slides were deparaffinized, then heated in a microwave processor for antigen retrieval in 10 mmol/L citrate buffer (pH 6.0) for 10 min. After blocking in 3% (v/v) bovine serum albumin, slides were incubated at 4°C overnight with the primary antibody (anti-CD26 mAb) and washed with PBS and the secondary antibody was labeled with biotin and applied for 30 min. Streptavidin-LSA amplification method was carried out for 30 min followed by peroxidase/diaminobenzidine substrate/chromagen. The slides were counterstained with hematoxylin. Two different pathologists checked the validity of the obtained results. All human specimens were obtained from Department of Pathology, Keio University (Tokyo, Japan), and informed consents were obtained from all patients according to the format of the institutional review board.

**Depletion of endogenous CD26.** To deplete endogenous CD26, small interfering RNA (siRNA) oligo-targeting CD26 cDNA (accession no. NM\_001935) was made according to the design site of TAKARA BIO;<sup>5</sup> sense: 5'-GAAAGGUGUCAGUACUAUU TT-3', antisense: 3'-TT CUUUCACAGUCAUGAUAA-5', with scrambled control of small interfering RNA oligo-targeting human Cas-L; sense: 5'-UAAUUAGG-GUCGGUAAAC TT-3', antisense: 3'-TT AUUAAUCCAGCCCCA-UUUG-5' being used as control. CD26 siRNA oligo (siCD26) was transfected using TransIT-TKO transfection reagent (Mirus Bio Corporation) according to the manufacturer's protocol.

**SDS-PAGE and immuno-blotting.** Preparation of whole-cell lysates, cell fractionations, and SDS-PAGE were done as described elsewhere (23).

**Antibody-dependent cell-mediated cytotoxicity.** The capacity of mAb to induce effector cell-dependent lysis of tumor cells was evaluated in Calcein-AM-release assay. Healthy donor natural killer cells were isolated from peripheral blood mononuclear cells by NK Cell Isolation kit II Miltenyi Biotec (Bergisch Gladbach) and used as effector cells. Target cells ( $1 \times 10^6$ ) were labeled with 10  $\mu$ mol/L Calcein-AM (Dojindo) shaking conditions at 37°C for 1 h. Cells were washed thrice with PBS and were resuspended in culture medium ( $1 \times 10^5$  cells/mL). Labeled cells were dispensed in 96-well U-bottomed plates ( $5 \times 10^3$  in 50  $\mu$ L/well) and preincubated (37°C, 30 min) with 50  $\mu$ L of 7-fold serial dilutions of humanized anti-CD26 mAb or 14D10 in culture medium, ranging from 0.1 pg/mL to 0.1 mg/mL (final concentrations). Culture medium was added instead of mAb to determine the spontaneous Calcein-AM release, with Triton X-100 (1% final concentration) being added to determine the maximal Calcein-AM release. Thereafter, human effector cells (HuEC) were added to the wells ( $5 \times 10^5$  cells per well) and cells were incubated at 37°C overnight. Supernatants were then collected for measurement of the Calcein-AM release. Percentage of specific lysis was calculated using the following formula: % specific lysis = (experimental release - spontaneous release)/(maximal release - spontaneous release)  $\times$  100; where maximal release was determined by adding Triton X-100 to target cells and spontaneous release was measured in the absence of sensitizing Abs and effector cells.

**Complement-dependent cytotoxicity.** Complement-dependent cytotoxicity (CDC) assay was done as described previously (24). Target cells were dispensed in 96-well U-bottomed plates ( $1 \times 10^5$  cells per well) incubated with various concentrations of mAbs at 4°C for 30 min. Subsequently, human serum was added and cells were incubated at 37°C for 2 h. Evaluation of CDC-specific cell death along with antibody-dependent cell-mediated cytotoxicity (ADCC)-specific cell death was assessed by Annexin V-FITC Apoptosis Detection kit (BioVision) and detection of activated caspase-3.

**Assessment of antitumor activity of humanized anti-CD26 mAb in effector-depleted SCID mice.** All *in vivo* studies were approved by the Institute Animal Care and Use Committee. Six-week-old female NOD-SCID mice were purchased from Charles River (Kanagawa, Japan) and were pretreated with anti-asialo-GM1 polyclonal antisera 25% (v/v; WAKO) i.p. 1 day before mAb treatment.

<sup>5</sup> <http://www.takara-bio.co.jp/RNAi.htm>

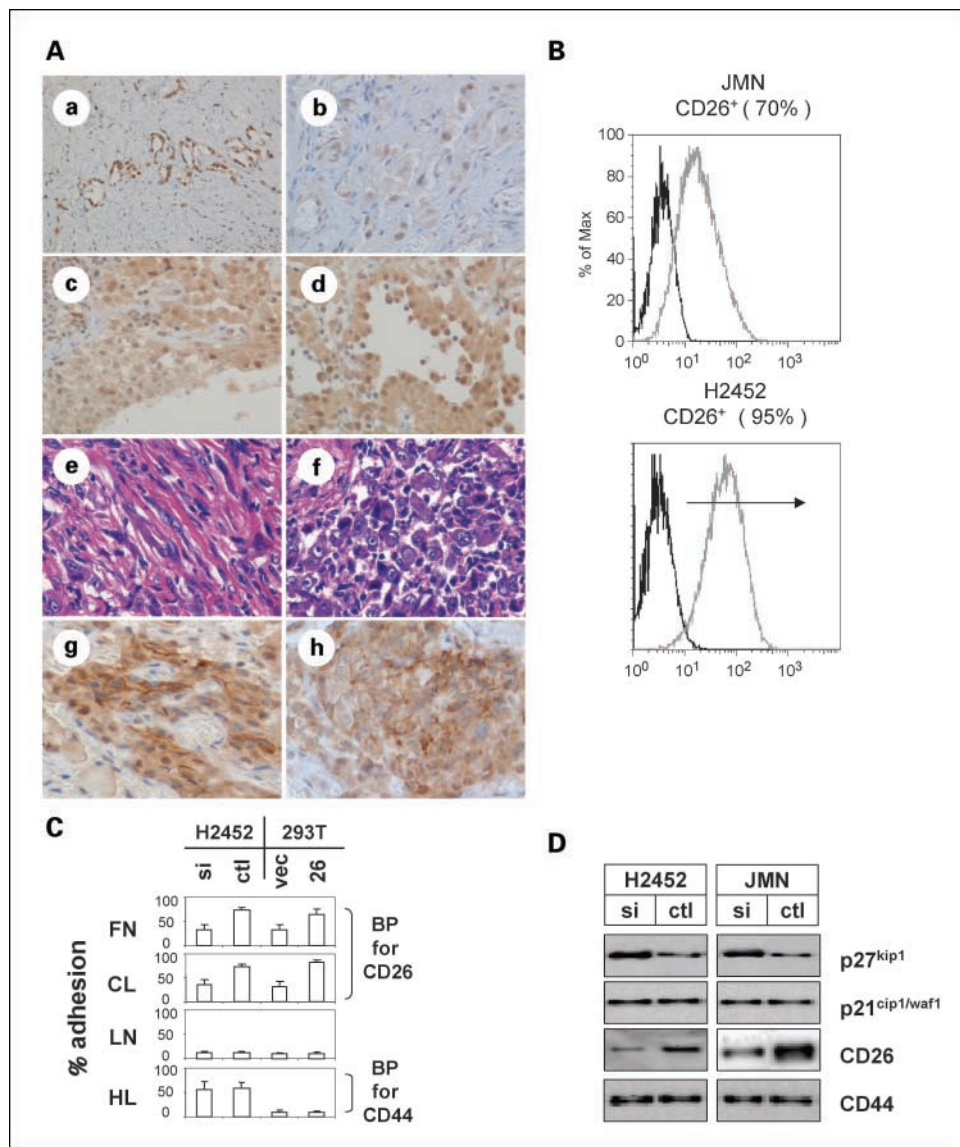


**Fig. 1.** Expression and functional role of CD26 in malignant mesothelioma. **A**, immunohistochemical localization of CD26 in adenomatoid tumor, reactive mesothelial cells and malignant mesothelioma. *a*, CD26 in adenomatoid tumor; *b*, CD26 in reactive mesothelial cells; *c*, CD26 in localized malignant mesothelioma; *d*, CD26 in well-differentiated papillary malignant mesothelioma; *e* and *f*, H&E stain in diffuse malignant mesothelioma; *g* and *h*, CD26 in diffuse malignant mesothelioma. Diffuse malignant mesothelioma specimens are showing biphasic features of sarcomatous malignant mesothelioma (*f, h*) and epithelial malignant mesothelioma (*g, i*). Indicated panels are representative of 12 consecutive specimens. Original magnification,  $\times 100$ . **B**, surface expression of CD26 on mesothelioma cell lines was analyzed by flow cytometry. Gray line, CD26 histograms were obtained by staining mouse anti-CD26mAb (14D10) followed by staining with rabbit anti-mouse IgG FITC conjugate; black line, control histograms represent back ground fluorescence obtained by staining of isotype-matched control mAb (2H4). **C**, adhesive property of CD26 to ECM. CD26-depleted NCI-H2452 (*si*), scrambled control oligo-transfected NCI-H2452 (*ctl*), pEB6 vector-transfected 293T (*vec*), or pEB6-CD26-transfected 293T (26) were plated onto 60-mm dishes ( $2 \times 10^6$  cells per dish) coated with fibronectin (FN), collagen I (CL), laminin (LN), or hyaluronan (HL) and cultured for 18 h. Fibronectin and collagen I are binding proteins (BP) to extracellular region of CD26, with hyaluronan being binding protein for CD44. The adhesive ability of cancer cells was expressed as the mean number of cells that had attached to the bottom surface of the dish. Columns, number of cells per field of view; bars, SD. Values for adhesion were determined by calculating the average number of adhesive cells per squared millimeters over three fields per assay and expressed as an average of triplicate determinations. Adhesive cells (%): adhesive cells/adhesive cells + nonadhesive cells. **D**, depletion of CD26 elicits up-regulation of p27<sup>kip1</sup>. NCI-H2452 cells and JMN cells were transfected with siRNA oligo (*si*) of CD26 or control oligo (*ctl*). At 48 h after transfection, cells were harvested, lysed, and subjected to SDS-PAGE, then probed by specific antibody to p27<sup>kip1</sup>, p21<sup>cip1/waf1</sup>, CD26, and CD44.

To assess the effect of humanized anti-CD26 mAb against tumorigenicity, JMN cells ( $1 \times 10^6$ ) were inoculated s.c. into the left flank of mice. Mice were treated with intratumoral injection of isotype-matched control mAb and 5F8, 14D10, or humanized anti-CD26 mAb (10  $\mu$ g per each injection) on the 14th day after cancer cell inoculation when the tumor mass became visible (5 mm in size). Each mAb was given thrice per week. Tumor-bearing mice were then monitored for tumor development and progression. Tumor size was determined by caliper measurement of the largest (*x*) and smallest (*y*)

perpendicular diameters and was calculated according to the formula  $V = \pi/6 \times xy^2$ .

To assess the effect of humanized anti-CD26 mAb against tumor dissemination, JMN cells ( $1 \times 10^5$ ) were injected i.v. via tail vein. Thereafter, mice were treated with i.v. injection of isotype-matched control mAb and 5F8, 14D10, or humanized anti-CD26 mAb (10  $\mu$ g per each injection), starting on the day of cancer cell injection. Each mAb was given thrice per week. Cumulative proportion survival was assessed by Kaplan-Meier.

**Table 1.** CD26 expression profile in patient samples

Patient no.	Gender/Age	Origin	Histology	CD26	
				CS	C
1	M/55	Pleura	RMC	-	±
2	F/63	Pleura	RMC	-	±
3	M/58	Pleura	RMC	-	±
4	F/39	Ovary	AT	-	+
5	F/5	Ovary	AT	-	±
6	M/67	Pleura	MM	+	++
7	M/60	Pleura	MM	++	+++
8	M/49	Pleura	MM	+	++
9	F/74	Pleura	MM	-	++
10	M/50	Pleura	MM	++	++
11	M/77	Pleura	MM	+	+++
12	M/61	Pleura	MM	+	+++

Abbreviations: RMC, reactive mesothelial cell; AT, adenomatoid tumor; MM, malignant mesothelioma; CS, cell surface; C, cytoplasm.

**Assessment of antitumor activity of humanized anti-CD26 mAb in effector-present Balb mice.** Six-week-old female Balb mice were purchased from Charles River, and treatment with anti-asialo-GM1 polyclonal antisera was not introduced to preserve the binding of the mouse effector system.

To assess the effect of humanized anti-CD26 mAb against tumorigenicity, JMN cells ( $1 \times 10^6$ ) were inoculated s.c. into the left flank of mice. Mice were treated with intratumoral injection of isotype-matched control mAb and 5F8, 14D10, or humanized anti-CD26 mAb (10  $\mu$ g per each injection) on the 14th day after cancer cell inoculation when the tumor mass became visible (5 mm in size). Each mAb was given thrice per week. Tumor-bearing mice were then monitored for tumor development and progression. Tumor size was determined by caliper measurement of the largest (x) and smallest (y) perpendicular diameters and was calculated according to the formula  $V = \pi/6 \times xy^2$ . On the 35th day after the first mAb treatment, all mice were euthanized to assess the microscopic feature of resected specimens in s.c. tumorigenicity model.

To assess the effect of humanized anti-CD26 mAb against tumor dissemination, JMN cells ( $1 \times 10^5$ ) were i.v. injected via tail vein. Thereafter, mice were treated with i.v. injection of isotype-matched control mAb or humanized anti-CD26 mAb (10  $\mu$ g per each injection) starting on the day of cancer cell injection. Each mAb was given thrice per week. Cumulative proportion of survival was assessed by Kaplan-Meier. To further assess the effect of humanized anti-CD26 mAb on distant metastasis formation, treated mice were euthanized and multiple metastasis formation in the lung and liver was calculated in another tumor dissemination model. JMN cells ( $1 \times 10^5$ ) were injected i.v. into mice in each group. Mice were treated with i.v. injection of isotype-matched control mAb (lane 1,  $n = 4$ ), 5F8 (lane 2,  $n = 4$ ), 14D10 (lane 3,  $n = 4$ ), or humanized anti-CD26 mAb (lane 4,  $n = 4$ ) on the day of cancer cell injection. Each mAb was given thrice per week. On the 35th day after cancer cell injection, mice were euthanized and multiple metastasis formation in the lung and liver was calculated.

**Construction of HuEC-engrafted mice and assessment of antitumor activity in NOD/Shi-scid. IL-R $\gamma$ <sup>null</sup> mice.** NOD/Shi-scid. IL-R $\gamma$ <sup>null</sup> (NOG mice) were obtained from Central Institute for Experimental Animals. Human peripheral blood mononuclear cells were isolated from the peripheral blood of a healthy donor using Lymphoprep (AXIS-SHIELD) and were used as HuEC. Thereafter, HuEC ( $5 \times 10^6$  cells) were injected i.p. in a volume of 0.2 mL suspended in PBS into NOG-SCID mice under sterile conditions. The mice were pretreated with a 0.2 mL

anti-asialo-GM1 polyclonal antisera 25% (v/v; WAKO) given i.p. 1 day before HuEC injection. NCI-H2452 cells ( $5 \times 10^4$ ) were injected i.p. into SCID mice engrafted with human HuEC 1 day after HuEC injection. One, three, and five days later, humanized anti-CD26 mAb were injected i.p. Mice were observed daily to monitor for death due to ascites tumor development. Cumulative proportion of survival was assessed by Kaplan-Meier.

## Results

**Cell surface CD26 is highly expressed on human malignant mesothelioma.** We first evaluated CD26 expression level on surgically resected human malignant mesothelioma tissues from patients. Twelve consecutive surgically resected specimens from the primary sites were examined for cell surface CD26 expression. CD26 was highly expressed on all malignant mesothelioma tissues (Fig. 1A; Table 1). In adenomatoid tumor or reactive mesothelial cells, CD26 expression was very weak (Fig. 1A-a,b). In contrast, CD26 was highly expressed in various pathologic types of malignant mesothelioma, including localized malignant mesothelioma, well-differentiated papillary malignant mesothelioma, and diffuse malignant mesothelioma (Fig. 1A-c to h). These results suggested that CD26 is highly expressed in malignant mesothelioma but not in benign mesothelial tissues.

**CD26 plays a role in cell adhesion to ECM.** Malignant mesothelioma cell lines, JMN and NCI-H2452, exhibited high-surface CD26 expressions (Fig. 1B).

Because CD26 has been described previously to play a role in cell adhesion to the ECM proteins (13, 25), we examined whether CD26 plays a role in cellular interaction with the ECM. As seen in Fig. 1C, NCI-H2452 that were depleted of endogenous CD26 using siRNA oligo showed significant loss of CD26 binding to ECM proteins, including fibronectin and collagen I. In contrast to these results, depletion of CD26 did not alter binding to laminin (an ECM protein lacking binding ability to CD26) or hyaluronan (a ligand for CD44; Fig. 1C). In further support of these findings, 293T cells transfected with full-length CD26 cDNA subcloned into pEB6 vector showed higher binding ability to fibronectin and collagen I than control pEB6-transfected 293T cells (Fig. 1C). Moreover, depletion of CD26 was associated with the up-regulation of p27<sup>kip1</sup> (Fig. 1D). These findings thus suggested that CD26 serves as a binding molecule to distinct ECM proteins and that contact inhibition may play a contributing role to the observed CD26 depletion-mediated up-regulation of p27<sup>kip1</sup> associated with CD26 depletion (26, 27).

**Anti-CD26 mAb perturbs cellular binding to ECM.** Because CD26 proved to be an ECM-binding protein, we further evaluated whether anti-CD26 mAbs disrupt cellular adhesion to ECM. For this purpose, isotype-matched control mAb and 5F8, 14D10, and humanized anti-CD26 mAb were evaluated for potential disruption to cellular adhesion to ECM. As seen in Fig. 2A, JMN cells treated with 14D10 and humanized anti-CD26 mAb had decreased binding to fibronectin and collagen I, whereas control mAb and 5F8 (anti-CD26 mAb without biological function) did not influence binding to fibronectin and collagen I. Moreover, 14D10 and humanized anti-CD26 mAb transmitted direct growth inhibition to JMN cells by *in vitro* proliferation assay in a dose-dependent manner, with humanized anti-CD26 mAb having a stronger antiproliferative

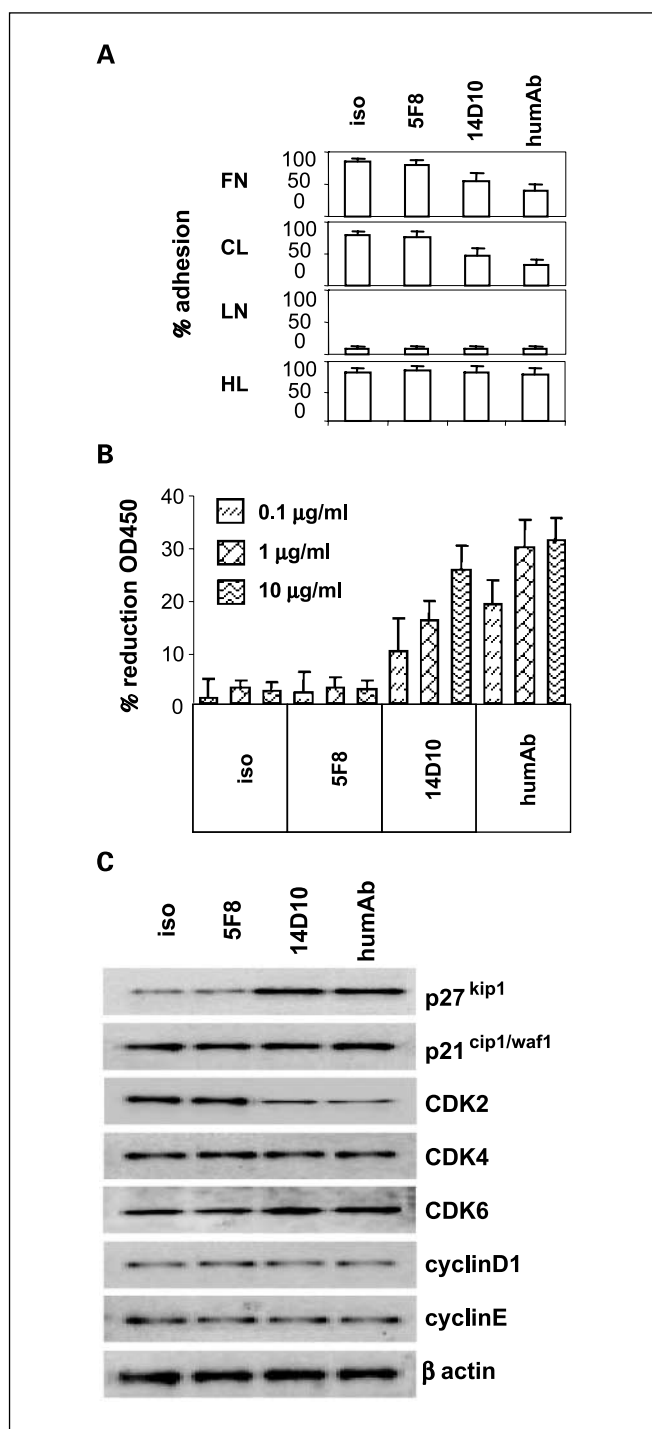


**Fig. 2.** Inhibitory effect of anti-CD26 mAbs on malignant mesothelioma proliferation. **A**, effect of anti-CD26 mAb on cell adhesion to ECM. JMN cells treated with isotype-matched control mAb (*iso*), 5F8, 14D10, or humanized anti-CD26 mAb (*humAb*) were plated onto 60-mm dishes ( $2 \times 10^6$  cells per dish) coated with fibronectin, collagen I, laminin, or hyaluronan and cultured for 18 h. Adhesive cells (%): adhesive cells/adhesive cells + nonadhesive cells. **B**,  $5 \times 10^3$  cells per well of JMN were incubated in 96-well plates in the presence of either isotype-matched control mAb, 5F8, 14D10, or humanized anti-CD26 mAb. After 24 h of antibody treatment, water-soluble formazan dye upon bioreduction in the presence of an electron carrier, 1-methoxy-5-methylphenazinium, was measured at 450 nm using a microplate reader as described in Materials and Methods, and growth inhibitory ratio was calculated as percentage reduction of absorbance 450 nm. **C**, JMN cells were treated with isotype-matched control mAb, 5F8, 14D10, or humanized anti-CD26 mAb. At 18 h after antibody administration, cells were harvested, lysed, and subjected to SDS-PAGE, then probed by specific antibody to p27<sup>kip1</sup>, p21<sup>cip1/waf1</sup>, CDK2, CDK4, CDK6, cyclinD1, cyclinE, and  $\beta$ -actin.

effect than 14D10 (Fig. 2B). Importantly, 14D10 and humanized anti-CD26 mAb induced up-regulation of p27<sup>kip1</sup> and down-regulation of CDK2. These results suggested that both 14D10 and humanized anti-CD26 mAb dynamically transmit contact inhibition-related growth inhibition via up-regulation of p27<sup>kip1</sup> and down-regulation of CDK2.

**Humanization of anti-CD26 mAb results in ADCC.** Whereas both 14D10 and humanized anti-CD26 mAb had similar direct effect on cancer cells, our present studies emphasized the different biological effects of humanized anti-CD26 mAb compared with 14D10 through the use of ADCC assay with HuEC. When effector/target (E/T) ratio was held constant at 50, JMN cells treated with humanized anti-CD26 mAb showed specific lysis via ADCC in an antibody dose-dependent manner (Fig. 3A, left). Importantly, JMN cells treated with 14D10 did not show ADCC-specific lysis (Fig. 3A, left), suggesting that humanization of 14D10 to humanized anti-CD26 mAb results in the induction of potent ADCC activity via engagement of the human effector system. Moreover, as seen in Fig. 3A (right), humanized anti-CD26 mAb provoked ADCC-specific lysis in effector-dose-dependent manner. These results were also found when other CD26 positive malignant mesothelioma line besides JMN (NCI-H2452) was used as target cells (Table 2). These data suggested that humanized anti-CD26 mAb possesses a novel biological function other than the direct effect on target cells seen with 14D10, namely ADCC-specific lysis. To better characterize the humanized anti-CD26 mAb-mediated ADCC, apoptosis assays using propidium iodide-annexin V staining and detection of cleaved caspase-3 were used. In these assays, cross-linking method using anti-human IgG, Fc $\gamma$  fragment specific F(ab')<sub>2</sub> fragment of goat, and anti-mouse IgG, Fc $\gamma$  fragment specific F(ab')<sub>2</sub> fragment of goat were used as mimicry of human effectors to humanized anti-CD26 mAb and 14D10, respectively. As seen in Fig. 3B (top three panels), cross-linked humanized anti-CD26 mAb induced late apoptosis, whereas cross-linked 14D10 did not induce late and early apoptosis. Importantly, neither humanized anti-CD26 mAb nor 14D10-induced CDC using human complement (Fig. 3B). To further support these binding, only cross-linked humanized anti-CD26 mAb induced activation of caspase-3 in JMN cells, whereas neither cross-linked 14D10, humanized anti-CD26 mAb plus human complement, and 14D10 plus human complement induced activation of caspase-3 (Fig. 3C). These results therefore indicated that humanized anti-CD26 mAb elicits ADCC-specific lysis but not CDC-specific lysis.

**Humanized anti-CD26 mAb possesses direct in vivo anti-tumor effect on malignant mesothelioma cells.** Because we recently showed that 14D10 exhibits direct *in vivo* antitumor effect on solid tumors (24), we further examined whether humanized anti-CD26 mAb has similar *in vivo* antitumor effect. For this purpose, we used NOD-SCID mice, which lack functional B and T cells as well as most natural killer cell activity (28). To minimize the effect of mouse effector cells, NOD-SCID mice were pretreated by anti-asialo-GM1 polyclonal antisera before being subjected to humanized anti-CD26 mAb functional evaluation. As seen in Fig. 4A and B, humanized anti-CD26 mAb and 14D10 reduced the tumorigenicity of s.c. inoculated JMN, with humanized anti-CD26 mAb being more potent in reducing tumor formation. These observed results suggested that humanized anti-CD26 mAb possesses stronger direct antitumor effect than 14D10. To

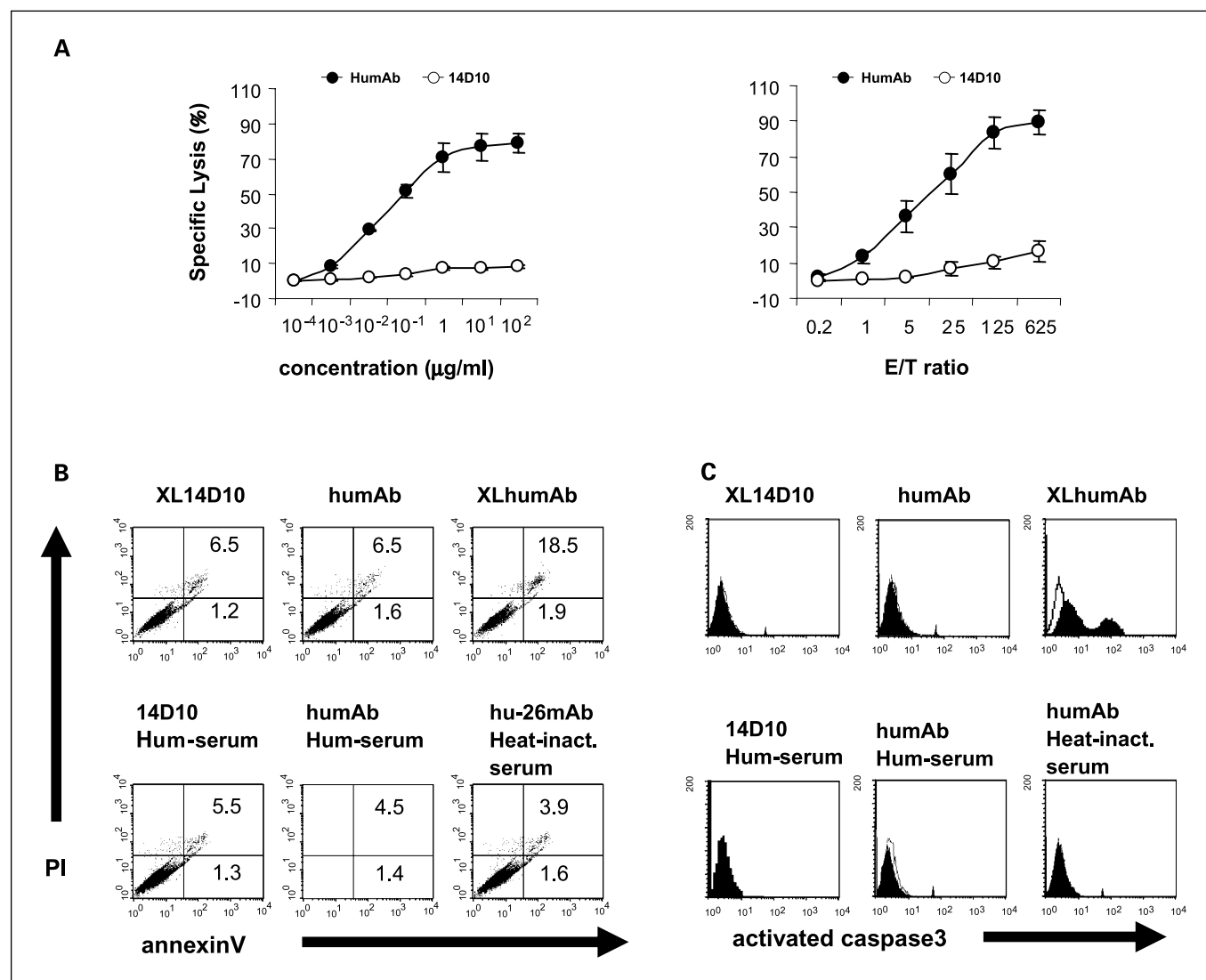


**Fig. 3.** ADCC-specific lysis of JMN cells by humanized anti-CD26 mAb. **A**, ADCC of humanized anti-CD26 mAb and 14D10 at the indicated concentrations on the X axis were examined (*left*). Effector/target (E/T) ratio was held constant at 50. ADCC of humanized anti-CD26 mAb and 14D10 in the presence of varying effector/target ratios were examined (*right*). Concentrations of mAbs were held constant at 5 µg/mL. Natural killer cells from healthy donor were used as effector cells. **B**, as a mimicry of effector cells in ADCC effects, cross-linking (XL) method of humanized anti-CD26 mAb and 14D10 was used. Top, cross-linked 14D10, intact humanized anti-CD26 mAb, cross-linked humanized anti-CD26 mAb, respectively. To examine the CDC, human serum was used. Bottom, 14D10 with serum, humanized anti-CD26 mAb with serum, and humanized anti-CD26 mAb with heat-inactivated serum. X axis, annexinV; Y axis, propidium iodide (PI). **C**, activated caspase-3 was evaluated in JMN cells pretreated with the cross-linked 14D10, intact humanized anti-CD26 mAb, cross-linked humanized anti-CD26 mAb, respectively (*top*), or in JMN cells pretreated with the 14D10 plus serum, humanized anti-CD26 mAb plus serum, and humanized anti-CD26 mAb plus heat-inactivated serum, respectively (*bottom*). X axis, activated caspase 3, Y axis, relative cell markers.

further examine the direct antitumor activity of humanized anti-CD26 mAb on tumor dissemination, we examined the effect of i.v.-given antibodies in a JMN xenograft model. As seen in Fig. 4C, humanized anti-CD26 mAb and 14D10 enhanced mouse survival when both antibodies were given i.v., with humanized anti-CD26 mAb being more efficient in promoting survival. All together, these observed results suggested that humanized anti-CD26 mAb is more potent than 14D10 in its direct antitumor activity.

*Mouse effector system may potentiate antitumor effect of anti-CD26 mAb.* While both humanized anti-CD26 mAb and 14D10 showed direct *in vivo* antitumor effect, we next examined the potential involvement of mouse effector system in anti-CD26 mAb activity induced antitumor effect. For this

purpose, we used Balb mice which possess robust natural killer cell activity. As seen in Fig. 5A, humanized anti-CD26 mAb and 14D10 reduced the tumorigenicity of s.c.-inoculated JMN. It should be noted that both 14D10 and humanized anti-CD26 mAb reduced tumor formation in the presence of mouse effector system (Fig. 5A). As seen in Fig. 5B, both humanized anti-CD26 mAb and 14D10-treated tumors showed resultant dead tissues upon microscopic analyses. These results suggested that both humanized anti-CD26 mAb and 14D10 used the mouse effector system in marked contrast with the observed differences between humanized anti-CD26 mAb and 14D10 in a mouse effector-depleted xenograft model. Additional studies using i.v. administration of JMN cells showed that i.v. injection of humanized anti-CD26 mAb effectively enhanced mouse

**Table 2.** Specific lysis by humanized anti-CD26 mAb in human malignant mesothelioma lines

MFI	JMN	NCI-H2452
CD26	68	56
% ADCC lysis	67	65

Abbreviations: MFI, mean fluorescent intensity; % ADCC lysis, percentage of ADCC-specific lysis.

survival in the presence of mouse effector system (Fig. 5C). Importantly, formation of distant JMN was similarly inhibited by both humanized anti-CD26 mAb and 14D10 (Fig. 5D). These data indicated that mouse effector system potentiates the anti-CD26 mAb-mediated direct antitumor effect.

**Human effector system may potentiate antitumor effect of humanized anti-CD26 mAb.** We next evaluated the potential involvement of human effector system in anti-CD26 mAb induced antitumor effect. For this purpose, NOG mice which have significant defects in T, B, and natural killer cell activities were used in a NCI-H2452 xenograft model construction. Human peripheral blood mononuclear cells were used as HuEC in this *in vivo* model. To completely deplete mouse effector system, NOG mice were pretreated with anti-asialo-GM1 antisera 1 day before i.p. HuEC implantation. As seen in Fig. 6, i.p. administration of humanized anti-CD26 mAb drastically enhanced NCI-H2452 xenograft mouse survival in the absence of HuEC. It should be noted that while 14D10 also enhanced mouse survival, its effect was much weaker than humanized anti-CD26 mAb in the absence of HuEC (Fig. 6). These results suggested that humanized anti-CD26 mAb possesses stronger direct antitumor effect. Importantly, in the presence of HuEC, the antitumor effect of humanized anti-CD26 mAb was exaggerated, whereas the antitumor effect of 14D10 was not altered significantly (Fig. 6). All together these observed results suggested that CD26 is an appropriate molecular target for mesothelioma therapy and humanized anti-CD26 mAb regulates tumor growth by at least two distinct mechanisms of action through its direct antitumor activity, as well as its ability to engage human effector system.

## Discussion

In this study, we show the antitumor effect of anti-CD26 mAb in an *in vitro* and *in vivo* model. Importantly, our study suggests that humanization of anti-CD26 mAb yields additive antitumor effect to contact inhibition associated with p27<sup>kip1</sup> induction. Our study also indicates the functional role of CD26 as a binding protein to ECM in human malignant mesothelioma.

Immunohistologic analysis indicates that human malignant mesothelioma cells express high level of surface CD26 than nonmalignant tissue, suggesting that CD26 may play a role in cancer growth and progression. It should be noted that depletion of endogenous CD26 in NCI-H2452 using siRNA oligo results in significant loss of binding to ECM, including fibronectin and collagen I. Moreover, 293T cells transfected with full-length CD26 cDNA exhibit higher binding affinity to fibronectin and collagen I than control mock-transfected 293T

cells. Moreover, depletion of CD26 leads to the up-regulation of p27<sup>kip1</sup>. These findings thus suggest that CD26 is involved in cancer cell adhesion to ECM and that contact inhibition may play a contributing role to the observed CD26 depletion-mediated up-regulation of p27<sup>kip1</sup>. Of note is the fact that it has

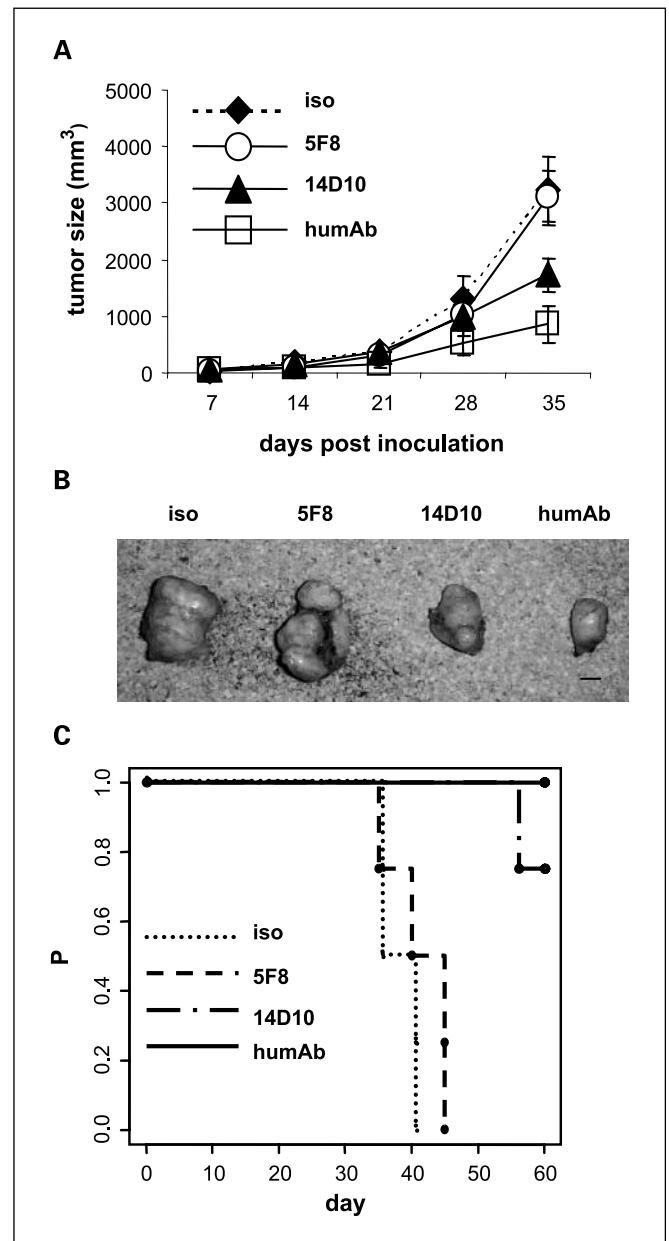


**Fig. 4.** *In vivo* direct effect of humanized anti-CD26 mAb: ADCC depletion model. Six-week-old female NOD-SCID mice were pretreated with anti-asialo-GM1 polyclonal antisera 1 d before treatment. **A**, effect of humanized anti-CD26 mAb in s.c. tumorigenicity was evaluated. JMN cells ( $1 \times 10^6$ ) were inoculated s.c. into the left flank of mice. Mice were treated with intratumoral injection of isotype-matched control mAb ( $n = 4$ ), 5F8 ( $n = 4$ ), 14D10 ( $n = 4$ ), or humanized anti-CD26 mAb ( $n = 4$ ) on the 14th day after cancer cell inoculation when the tumor mass became visible (5 mm in size). Each mAb was given at 10  $\mu$ g per injection at thrice per week. **B**, representative resected specimens in s.c. tumorigenicity model on 35th day after first mAb treatment. **C**, effect of humanized anti-CD26 mAb in tumor dissemination model was evaluated. JMN cells ( $1 \times 10^5$ ) were injected i.v. into mice in each group. Mice were treated with i.v. injection of isotype-matched control mAb ( $n = 4$ ), 5F8 ( $n = 4$ ), 14D10 ( $n = 4$ ), or humanized anti-CD26 mAb ( $n = 4$ ) on the day of cancer cell injection. Each mAb was given at 10  $\mu$ g per injection at thrice per week.

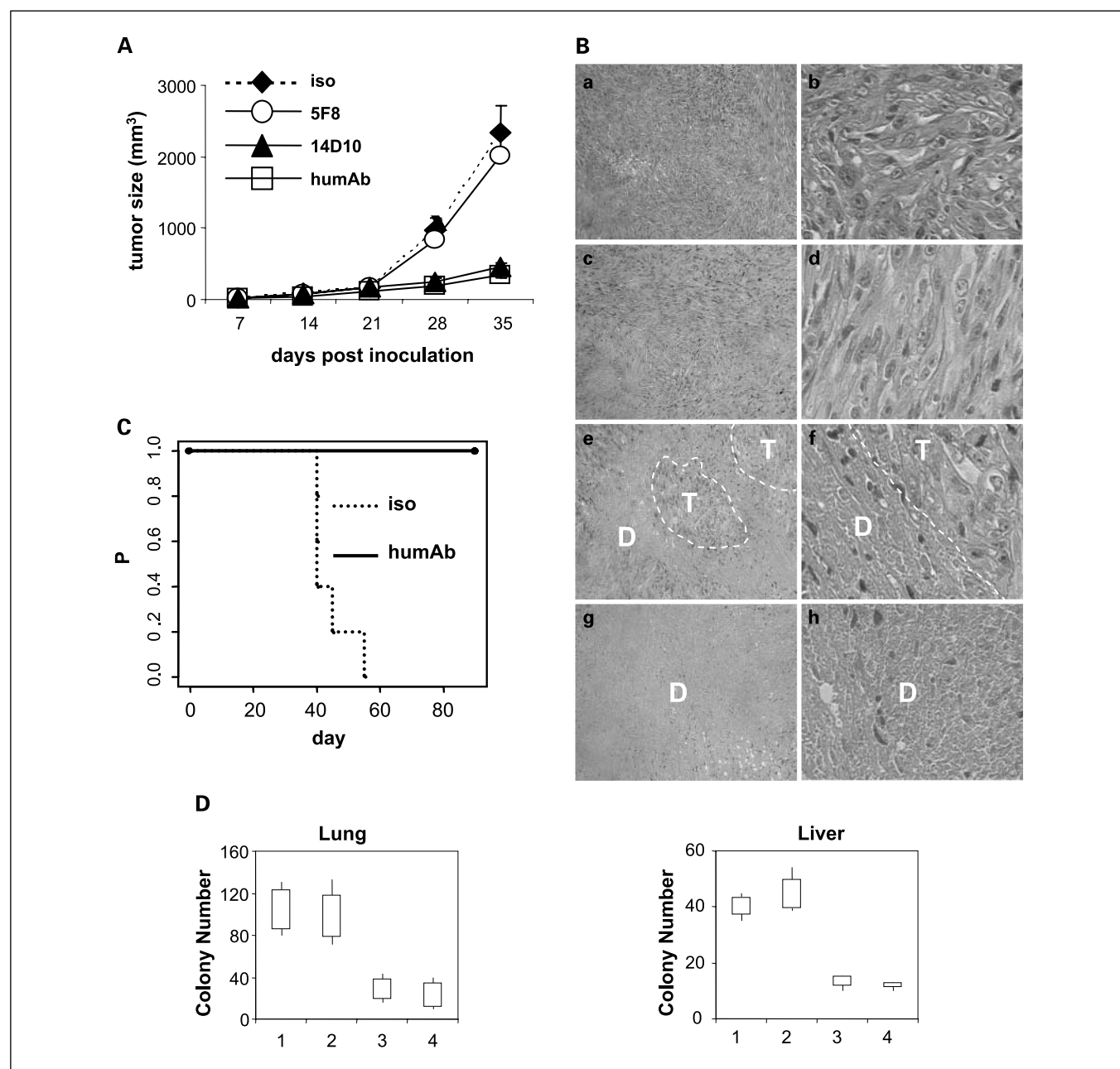


**Fig. 5.** *In vivo* direct and indirect effect of humanized anti-CD26 mAb: mouse ADCC presence model. Six-week-old female Balb mice were enrolled in this experiment. **A**, effect of humanized anti-CD26 mAb in s.c. tumorigenicity was evaluated. JMN cells ( $1 \times 10^6$ ) were inoculated s.c. into the left flank of mice. Mice were treated with intratumoral injection of isotype-matched control mAb ( $n = 4$ ), 5F8 ( $n = 4$ ), 14D10 ( $n = 4$ ), or humanized anti-CD26 mAb ( $n = 4$ ) on the 14th day after cancer cell inoculation when the tumor mass became visible (5 mm in size). Each mAb was given at 10  $\mu$ g per injection at thrice per week. **B**, representative H&E stain feature of resected specimens on 35th day after first mAb treatment. **a**, isotype-matched control mAb ( $\times 100$ ); **b**, isotype-matched control mAb ( $\times 600$ ); **c**, 5F8 ( $\times 100$ ); **d**, 5F8 ( $\times 600$ ); **e**, 14D10 ( $\times 100$ ); **f**, 14D10 ( $\times 600$ ); **g**, humanized anti-CD26 mAb ( $\times 100$ ); **h**, humanized anti-CD26 mAb ( $\times 600$ ). White broken line, the line between tumor (T) and dead tissue (D). **C**, effect of humanized anti-CD26 mAb in tumor dissemination model was evaluated. JMN cells ( $1 \times 10^5$ ) were injected i.v. into mice in each group. Mice were treated with i.v. injection of isotype-matched control mAb ( $n = 5$ ) or humanized anti-CD26 mAb ( $n = 5$ ) on the day of cancer cell injection. Each mAb was given at 10  $\mu$ g per injection at thrice per week. **D**, effect of humanized anti-CD26 mAb onto distant metastasis formation in tumor dissemination model was evaluated. JMN cells ( $1 \times 10^5$ ) were injected i.v. into mice in each group. Mice were treated with i.v. injection of isotype-matched control mAb (lane 1,  $n = 4$ ), 5F8 (lane 2,  $n = 4$ ), 14D10 (lane 3,  $n = 4$ ), or humanized anti-CD26 mAb (lane 4,  $n = 4$ ) on the day of cancer cell injection. Each mAb was given at 10  $\mu$ g per injection at thrice per week. On 35th day after cancer cell injection, mice were euthanized and multiple metastasis formation in the lung and liver was calculated.

been previously reported that p27<sup>kip1</sup> is up-regulated during contact inhibition (26).

Both humanized anti-CD26 mAb and 14D10 display direct inhibition of malignant mesothelioma growth via p27<sup>kip1</sup> up-regulation and disruption of binding to ECM. Hence, our

results with these anti-CD26 monoclonal antibodies are consistent with those obtained from above small interfering RNA study, showing that both humanized anti-CD26 mAb and 14D10 have an antagonistic effect on the adhesive property of malignant mesothelioma.



Further examination of their effector functions associated with anti-CD26 mAb-mediated antitumor effect indicates that humanized anti-CD26 mAb, but 14D10, elicits ADCC-induced cell lysis. Cross-linking of humanized anti-CD26 mAb results in an accumulation of annexin V-positive and propidium iodide-positive population and cleavage of activated caspase-3. These data suggest that humanization of anti-CD26 mAb elicits greater contribution from ADCC in addition to a direct antitumor effect. Meanwhile, the precious reason why humanized anti-CD26 mAb does not induce CDC activity is not clear at the moment. One of the reasons is the high-surface expression of DAF and CD59, which are antagonistic to human complement proteins (data not shown). Or, our *in vitro* system may not be appropriate for the induction of CDC activation.

*In vivo* study with NOD-SCID mice shows that humanized anti-CD26 mAb and 14D10 reduce the tumorigenicity of s.c.-inoculated JMN cells, suggesting that humanized anti-CD26 mAb possesses direct antitumor effect as well. Our results also suggest that humanized anti-CD26 mAb is more potent in reducing tumor formation, possibly due to its higher binding affinity to CD26 than 14D10.

Meanwhile, *in vivo* study with Balb mice show that humanized anti-CD26 mAb and 14D10 are equally effective in reducing the tumorigenicity of s.c.-inoculated JMN cells. These data suggest that the mouse effector system may

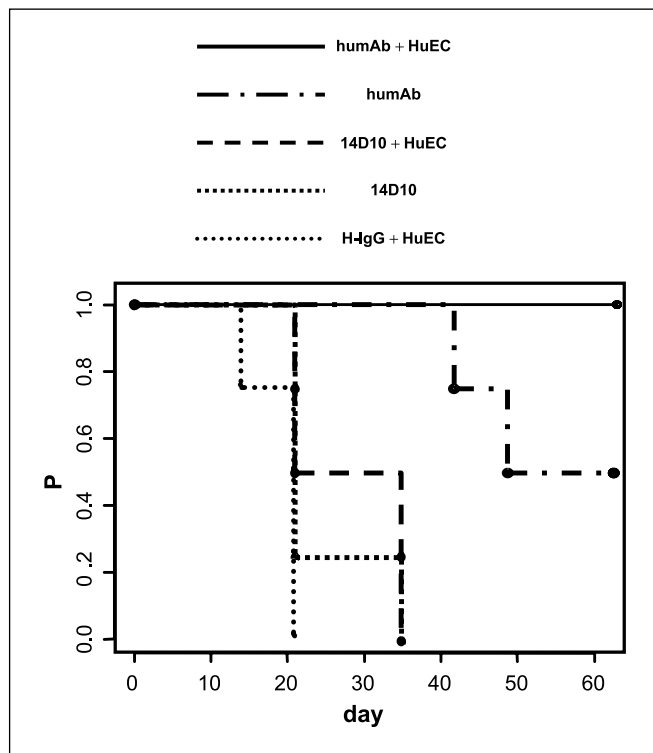


**Fig. 6.** *In vivo* direct and indirect effect of humanized anti-CD26 mAb: human ADCC presence model. Six-week-old female NOG-SCID mice were enrolled in this experiment. Mice were divided into two groups, HuECs-implanted group and HuEC-negative group, respectively. All mice were pretreated with anti-asialo-GM1 polyclonal antisera i.p. 2 d before HuEC implantation. HuEC were implanted i.p. with effector/target ratio of 10:1. JMN cells ( $1 \times 10^6$ ) were implanted 1 d after HuEC implantation into the peritoneal cavity of mice. The latter group was left untreated. All mice were treated with human normal IgG + HuEC (*H-IgG+HuEC*,  $n = 4$ ), 14D10 ( $n = 4$ ), 14D10 + HuEC ( $n = 4$ ), humanized anti-CD26 mAb ( $n = 4$ ), or humanized anti-CD26 mAb+HuEC (*humAb+HuEC*,  $n = 4$ ). Each mAb was given i.p. at 10  $\mu$ g per injection, 1, 3, and 5 d after cancer cell implantation.

potentiate the antitumor effect of 14D10 more than humanized anti-CD26 mAb. In fact, not only humanized anti-CD26 mAb but also 14D10-treated tumor specimens from these mice exhibit a reduction of viable cells in tumor mass. It is also noteworthy that both humanized anti-CD26 mAb and 14D10 reduce the formation of distant metastasis, findings which may be partly explained from our *in vitro* results that CD26 serves as a binding protein to distinct ECM proteins.

*In vivo* study with NOG-SCID mice which lack functional mice effectors show that dual-xenograft of HuEC plus target cells results in greater mouse survival than single xenograft of target cells when combined with humanized anti-CD26 mAb. These data clearly corroborate the *in vitro* data, suggesting that humanized anti-CD26 mAb induces a biphasic antitumor action with a human effector system.

CD26 status may be altered in cancer and may have an effect on the growth and metastatic potential of various tumors. Absence of CD26 is associated with the development of some cancers, whereas presence of CD26 is associated with a more aggressive phenotype in other neoplasms. For example, in non-small cell lung cancer cell lines, cells transfected with CD26 develop morphologic changes, altered contact inhibition, and reduced ability for anchorage-independent growth (29). CD26 reexpression also correlates with increased p21<sup>cip2/waf1</sup> expression, leading to induction of apoptosis and cell cycle arrest in G<sub>1</sub> stage. Wesley et al. reported that CD26/dipeptidyl peptidase IV up-regulates the expression of CDKI p27<sup>kip1</sup> by 4-fold to 6-fold in CD26-transfected DU-145 metastatic prostate cancer cells compared with the parent and vector-transfected DU-145 cells (30). It is also reported that overexpression of CD26 in ovarian cancer leads to increased E-cadherin and tissue inhibitors of matrix metalloproteinases, resulting in decreased invasive potential (31). CD26/dipeptidyl peptidase IV thus functions as a tumor suppressor in the cases described above, and its down-regulation may contribute to the loss of growth control. In contrast, CD26 expression is associated with a more aggressive clinical course in T-cell large granular lymphocyte leukemia (32).

An earlier report indicated that CD26 and CD40L expression is mutually exclusive, with CD40L expressed on cells from more indolent diseases. Of note is that CD26 expression on T-cell LBL/ALL is associated with a worse survival (33). We now show that CD26 is highly expressed in malignant mesothelioma tissues and anti-CD26 mAb treatment and CD26 down-regulation by siRNA in CD26-positive malignant mesothelioma cell lines lead to contact inhibition and p27<sup>kip1</sup> up-regulation. Therefore in case of malignant tumors, such as T-cell lymphoma, and malignant mesothelioma, CD26 plays a role in tumor growth and may be involved in invasion and metastasis.

Malignant mesothelioma is an aggressive neoplasm with a dismal prognosis and is relatively unresponsive to chemotherapy. One study systematically reviewed evidence for chemotherapy effect from 1965 through June 2001 and found 83 studies with 88 treatment arms (34). Cisplatin was the most active single drug, and cisplatin with doxorubicin had the highest response rate (28.5% response rate; confidence interval, 21.3% to 35.7%). Since this report, results of a phase III randomized trial (using 448 chemotherapy naive patients with unresectable mesothelioma) involving the combination cisplatin/pemetrexed (an antimetabolite) or cisplatin alone have shown that medium survival is extended from 9.3 months in

patients treated with cisplatin to 12.1 months in patients treated with both agents (35). However, standard treatments for malignant mesothelioma are still not satisfactory in terms of survival; hence, there is an urgent need for novel therapeutic approaches for malignant mesothelioma.

Our data therefore indicate that the novel humanized anti-CD26 mAb is an effective therapeutic tool for cancer treatment including malignant mesothelioma, as it can use the human effector system to target cancer cells in addition to its direct antitumor effect.

## References

- Britton M. The epidemiology of mesothelioma. *Semin Surg Oncol* 2002;29:18–25.
- Connelly RR, Spirtas R, Myers MH, Percy CL, Fraumeni JF, Jr. Demographic patterns for mesothelioma in the United States. *J Natl Cancer Inst* 1987;78:1053–60.
- Ismaril-Khan R, Robinson LA, Williams CC, Jr., Garrett CR, Bepler G, Simon GR. Malignant Pleural Mesothelioma, a comprehensive review. *Cancer control* 2006;13:255–63.
- Pass H. Malignant pleural mesothelioma, surgical roles and novel therapies. *Clin Lung Cancer* 2001;3:102–17.
- Morimoto C, Schlossman SF. The structure and function of CD26 in the T-cell immune response. *Immunol Rev* 1998;161:55–70.
- Ishii T, Ohnuma K, Murakami A, et al. CD26-mediated signaling for T cell activation occurs in lipid rafts through its association with CD45RO. *Proc Natl Acad Sci U S A* 2001;98:12138–43.
- Ohnuma K, Yamochi T, Uchiyama M, et al. CD26 up-regulates expression of CD86 on antigen-presenting cells by means of caveolin-1. *Proc Natl Acad Sci U S A* 2004;101:14186–91.
- Yamochi T, Yamochi T, Aytac U, et al. Regulation of p38 phosphorylation and topoisomerase II $\alpha$  expression in the B-cell lymphoma line Jiyoye by CD26/dipeptidyl peptidase IV is associated with enhanced *in vitro* and *in vivo* sensitivity to doxorubicin. *Cancer Res* 2005;65:1973–83.
- Pro B, Dang NH. CD26/dipeptidyl peptidase IV and its role in cancer. *Histol Histopathol* 2004;19:1345–51.
- Iwata S, Morimoto C. CD26/dipeptidyl peptidase IV in context. The different roles of a multifunctional ectoenzyme in malignant transformation. *J Exp Med* 1999;190:301–6.
- Kehlen A, Lendeckel U, Dralle H, Langner J, Hoang-Vu C. Biological significance of aminopeptidase N/CD13 in thyroid carcinomas. *Cancer Res* 2003;63:8500–6.
- Kajiyama H, Kikkawa F, Suzuki T, Shibata K, Ino K, Mizutani S. Prolonged survival and decreased invasive activity attributable to dipeptidyl peptidase IV overexpression in ovarian carcinoma. *Cancer Res* 2002;62:2753–7.
- Cheng HC, Abdel-Ghany M, Pauli BU. A novel consensus motif in fibronectin mediates dipeptidyl peptidase IV adhesion and metastasis. *J Biol Chem* 2003;278:24600–7.
- Johnson RC, Zhu D, Augustin-Voss HG, Pauli BU. Lung endothelial dipeptidyl peptidase IV is an adhesion molecule for lung-metastatic rat breast and prostate carcinoma cells. *J Cell Biol* 1993;121:1423–32.
- Dang NH, Torimoto Y, Schlossman SF, Morimoto C. Human CD4 helper T cell activation: functional involvement of two distinct collagen receptors. *J Exp Med* 1990;172:649–52.
- Ohnuma K, Ishii T, Iwata S, et al. G<sub>1</sub>-S cell cycle arrest provoked in human T cells by antibody to CD26. *Immunology* 2002;107:325–33.
- Ho L, Aytac U, Stephens LC, et al. *In vitro* and *in vivo* antitumor effect of the anti-CD26 monoclonal antibody 1F7 on human CD30+ anaplastic large cell T-cell lymphoma Karpas 299. *Clin Cancer Res* 2001;7:2031–40.
- Inamoto T, Yamochi T, Ohnuma K, et al. Anti-CD26 monoclonal antibody-mediated G<sub>1</sub>-S arrest of human renal clear cell carcinoma Caki-2 is associated with retinoblastoma substrate dephosphorylation, cyclin-dependent kinase 2 reduction, p27(kip1) enhancement, and disruption of binding to the extracellular matrix. *Clin Cancer Res* 2006;12:3470–7.
- Usami N, Fukui T, Kondo M, et al. Establishment and characterization of four malignant pleural mesothelioma cell lines from Japanese patients. *Cancer Sci* 2006;97:387–94.
- Morimoto C, Torimoto Y, Levinson G, et al. 1F7, a novel cell surface molecule, involved in helper function of CD4 cells. *J Immunol* 1989;143:3430–9.
- Kobayashi S, Ohnuma K, Uchiyama M, et al. Association of CD26 with CD45RA outside lipid rafts attenuates cord blood T-cell activation. *Blood* 2004;103:1002–10.
- Tanaka J, Miwa Y, Miyoshi K, Ueno A, Inoue H. Construction of Epstein-Barr virus-based expression vector containing mini-oriP. *Biochem Biophys Res Commun* 1999;264:938–43.
- Sato K, Aytac U, Yamochi T, et al. CD26/dipeptidyl peptidase IV enhances expression of topoisomerase II $\alpha$  and sensitivity to apoptosis induced by topoisomerase II inhibitors. *Br J Cancer* 2003;89:1366–74.
- Prang N, Preithner S, Brischwein K, et al. Cellular and complement-dependent cytotoxicity of Ep-CAM-specific monoclonal antibody MT201 against breast cancer cell lines. *Br J Cancer* 2005;92:342–9.
- Dang NH, Torimoto Y, Schlossman SF, Morimoto C. Human CD4 helper T cell activation: functional involvement of two distinct collagen receptors, 1F7 and VLA integrin family. *J Exp Med* 1990;172:649–52.
- Suzuki E, Nagata D, Yoshizumi M, et al. Reentry into the cell cycle of contact-inhibited vascular endothelial cells by a phosphatase inhibitor. Possible involvement of extracellular signal-regulated kinase and phosphatidylinositol 3-kinase. *J Biol Chem* 2000;275:3637–44.
- Levenberg S, Yarden A, Kam Z, Geiger B. p27 is involved in N-cadherin-mediated contact inhibition of cell growth and S-phase entry. *Oncogene* 1999;18:869–76.
- Shultz LD, Schweitzer PA, Christianson SW, et al. Multiple defects in innate and adaptive immunologic function in NOD/LtSz-scid mice. *J Immunol* 1995;154:180–91.
- Wesley UV, Tiwari S, Hoghton AN. Role for dipeptidyl peptidase in tumor suppression of human non small cell lung carcinoma cells (NSCLC). *Int J Cancer* 2004;109:855–66.
- Wesley UV, McGroarty M, Homoyouni A. Dipeptidyl peptidase inhibits malignant phenotype of prostate cancer cells by blocking basic fibroblast growth factor signaling pathway. *Cancer Res* 2005;65:1325–34.
- Kajiyama H, Kikkawa F, Khin E, Shibata K, Ino K, Mizutani S. Dipeptidyl peptidase overexpression induces up-regulation of E-cadherin and tissue inhibitors of matrix metalloproteinases, resulting in decreased invasive potential in ovarian carcinoma cells. *Cancer Res* 2003;63:2278–83.
- Dang NH, Aytac U, Sato K, et al. T-large granular lymphocyte lymphoproliferative disorder: expression of CD26 as a marker of clinically aggressive disease and characterization of marrow inhibition. *Br J Haematol* 2003;121:857–65.
- Canbon A, Gloghini A, Zagonel V, et al. The expression of CD26 and CD40 ligand is mutually exclusive in human T-cell non-Hodgkin's lymphomas/leukemias. *Blood* 1995;86:4617–26.
- Berghmans T, Paesmans M, Lalami Y, et al. Activity of chemotherapy and immunotherapy on malignant mesothelioma: a systemic review of the literature with meta-analysis. *Lung Cancer* 2002;38:111–21.
- Vogelzang NJ, Rusthoven JJ, Symanowski J, et al. Phase study of pemetrexed in combination with cisplatin versus cisplatin alone in patients with malignant pleural mesothelioma. *J Clin Oncol* 2003;21:2629–30.